RSC Advances

PAPER

View Article Online
View Journal | View Issue

Check for updates

Cite this: *RSC Adv.*, 2026, **16**, 8889

A strategy combining UPLC fingerprint, chemometrics and quantitative analysis of multi-components by single-marker to control the quality of *Carpesium abrotanoides* L.

Jingxiao Yang, †[a] Yijia Zhang,†[a] Yuanqing Wang,[b] Xinyue Hu,[a] Jingjing Yu,[e] Ping Fu,[e] Shunxiang Li*[acd] and Jianye Yan*[acd]

Carpesium abrotanoides L. (CA), a dried whole herb from the Asteraceae family, features prominent heat-clearing and detoxifying properties. However, a rigorous criterion for evaluating the quality of CA has yet to be established. Therefore, the aim of this study was to conduct quality control research on CA by combining ultra-high-performance liquid chromatography (UPLC) Fingerprint, chemometrics and quantitative analysis of multi-components by a single-marker (QAMS) method. Through the fingerprint analysis of 17 batches of CA, a total of 19 common peaks were identified by UPLC-QTOF-MS, and 10 components were confirmed *via* reference standards, including 5 phenolic acids, 4 sesquiterpenoids, and 1 flavonoid component. 12 differential components were screened out through chemometric analysis by hierarchical clustering analysis (HCA), principal component analysis (PCA), and orthogonal partial least squares method-discriminant analysis (OPLS-DA). Using isochlorogenic acid A as the internal standard, relative correction factors were established for chlorogenic acid, caffeic acid, cynaroside, 11(13)-dehydroivaxillin, isochlorogenic acid C, 2,3,4,5-tetracaffeoyl-D-glucaric acid, 2-deoxy-4-*epi*-gaillardin, carabrone, and telekin, allowing for the quantification of 10 components. The QAMS and the external standard method (ESM) showed no substantial difference in their determination results, demonstrating the accuracy and reliability of the QAMS established with isochlorogenic acid A as the internal standard. The strategy combining fingerprint analysis, chemometrics, and QAMS proposed herein can control the quality of CA quickly and efficiently. This study lays a theoretical foundation for the quality control and clinical application of CA.

Received 4th January 2026
Accepted 6th February 2026

DOI: 10.1039/d6ra00067c

rsc.li/rsc-advances

Open Access Article. Published on 13 February 2026. Downloaded on 5/20/2026 7:02:52 PM.
This article is licensed under a Creative Commons Attribution-NonCommercial 3.0 Unported Licence.

1 Introduction

Carpesium abrotanoides L. (CA), a dried whole herb falling within the Asteraceae family, is broadly distributed in East Asia, spanning China, Korea, Japan, and Vietnam.[1] CA is mainly distributed in the regions of Southwest, East and Central China, as well as in Hebei Province. It is valued for its traditional pharmacological properties, such as heat-clearing, detoxification, phlegm resolution, insecticidal effects, and haemostasis, among others.[2] As a medicinal herb, it holds significant importance in traditional Chinese medicine due to its abundant phytochemical composition, low toxicity, and potent bioactivities.[3] Current studies have indicated that CA contains a variety of phytochemicals, including terpenoids, nitrogenous alkaloids, fatty acids, flavonoids, and alkanes[4,5] and exhibits a range of pharmacological activities, such as anti-inflammatory,[6,7] antiviral,[8] antitumor,[9–11] cytotoxic,[12,13] insecticidal,[14] and microbicidal[15] efficacies. In China, CA is a distinguished herb among the Tujia, Miao, Bai, and Tibetan ethnic groups, with clinical applications in toothache, gastric ulcers, furuncles, tonsillitis, bronchitis, bacterial infections, traumatic swelling, viral fevers, and anthelmintic treatment against Ascaris, Taenia, Ancylostoma, and Enterobius.[4,8,15,16] The unique efficacy of CA has been widely applied and recognized in long-term clinical medical practice. However, the lack of standard research on the medicinal material has seriously hindered the development of its industry. Currently, CA has not yet been included in the national pharmacopoeia, and the existing quality studies are limited, with relatively few single indicators for content determination.

[a]*Academy of Chinese Medical Sciences and School of Pharmacy, Hunan University of Chinese Medicine, Changsha 410208, China. E-mail: yanjy@hnucm.edu.cn*

[b]*College of Life Science and Technology, Central South University of Forestry and Technology, Changsha 410004, China*

[c]*Hunan Engineering Technology Research Center for Bioactive Substance Discovery of Chinese Medicine, Changsha 410208, China*

[d]*Hunan Province Sino-US International Joint Research Center for Therapeutic Drugs of Senile Degenerative Diseases, Changsha 410208, China*

[e]*Xiangxi Hongcheng Pharmaceutical Co., Ltd, Hunan Jishou, 416007, China*

† Equal contribution.

© 2026 The Author(s). Published by the Royal Society of Chemistry

Open Access Article. Published on 13 February 2026. Downloaded on 5/20/2026 7:02:52 PM.
This article is licensed under a Creative Commons Attribution-NonCommercial 3.0 Unported Licence.

In previous studies, nuclear magnetic resonance (NMR) techniques,[17–20] liquid chromatography-mass spectrometry (LC-MS),[3] and gas chromatography-mass spectrometry (GC-MS)[21] were mostly utilized for the qualitative analysis of the components in CA. Present quantitative studies are few and mainly centered around sesquiterpenoids using high-performance liquid chromatography (HPLC). For example, Liu Min *et al.* quantified the contents of 5 sesquiterpene components (11(13)-dihydrotelekint, telekin, carabrone, carabrol, and 2-deoxy-4-*epi*-gaillardin) in CA by HPLC.[22] However, there is an absence of pertinent quantitative analysis that simultaneously determines the sesquiterpenoid, phenolic acid, and flavonoid components in CA. UPLC is a prevalent quantitative analysis method characterized by simpler operation, lower running cost, and a shorter analysis cycle in comparison to NMR, LC-MS, and GC-MS. Combined with fingerprint technology, UPLC can not only efficiently separate and rapidly detect complex components but also establish an overall quality control mode through characteristic peak matching and similarity evaluation, providing a cost-efficient solution for the standardization research of traditional Chinese medicine quality. Meanwhile, UPLC has superior resolution, sensitivity, and analysis speed compared to traditional HPLC.[23] It has been widely applied in traditional Chinese medicine analysis.[23–27] Akin to that of most traditional Chinese medicines, the quality evaluation of CA is characterized by integrity and chemical diversity. Reliance on single-component markers (sesquiterpenoids) is inadequate to fully represent its multi-constituent profile.[28] Furthermore, up to now, few standardized methods for its quantitative analysis have been established, and the quality standard system remains incomplete. Thus, it is essential to develop a thorough quality control methodology integrating UPLC-fingerprinting and multi-component quantification of CA, guaranteeing the safety and efficacy of clinical applications.

Chromatographic fingerprinting, as an advanced chemical characterization method, can comprehensively represent the "holistic" and "complex" attributes of CA. Currently, it stands as the internationally accepted method in evaluating the quality of medicinal herbs.[29,30] QAMS (quantitative analysis of multi-components by single-marker) offers a cost-effective and rapid strategy to concurrently quantify multiple bioactives using a single reference standard. This method can substantially decrease experimental costs, shorten detection duration, effectively enhance practicality, and thus comprehensively control the quality of medicinal materials or plant products.[31,32] The novel QAMS method introduced in this study enables synchronous quantification of 10 components in CA, including sesquiterpenoids (11(13)-dehydroivaxillin, 2-deoxy-4-*epi*-gaillardin, carabrone, and telekin), phenolic acids (chlorogenic acid, caffeic acid, isochlorogenic acid A, isochlorogenic acid C, and 2,3,4,5-tetracaffeoyl-D-glucaric acid), and flavonoids (cynaroside), utilizing a single reference standard. This method can address the challenges posed by numerous reference standards for CA, which are typically hard to source and high in cost. The analytical strategy using UPLC technology to simultaneously determine the 10 components of CA is reported for the first time. By integrating the UPLC fingerprinting with QAMS, it is feasible to comprehensively evaluate various types of components in CA, such as sesquiterpenoids, phenolic acids, and flavonoids. This combination holds significant value for the thorough evaluation and control of CA quality.

Therefore, this study pioneered in establishing the UPLC fingerprint and QAMS, with 17 batches of CA medicinal materials as the research objects, to comprehensively characterize the chemical composition differences of CA. Furthermore, similarity and correlation analysis, chemometric methods, and quality fluctuation analysis were integrated to perform quality evaluation of CA. This strategy incorporates the UPLC fingerprint-chemometrics-QAMS method to offer theoretical support for the construction of the quality standardization system of CA and the screening of key markers.

2 Materials and methods

2.1 Chemicals and reagents

Chlorogenic acid (No. HR2311W2), isochlorogenic acid A (No. HS20112B1), 2,3,4,5-tetracaffeoyl-D-glucaric acid (No. HR6342W1), and cynaroside (No. HS09192B1) were all procured from Baoji Chenguang Biotechnology Co., Ltd (Baoji, China), with purity all ≥98%. Isochlorogenic acid C (No. WP23120802), carabrone (No. WP23110902), telekin (No. WP23110803), 11(13)-dehydroivaxillin (No. WP23111301), and 2-deoxy-4-*epi*-gaillardin (No. WP23111001) were all supplied by Sichuan Weikeqi Biotechnology Co., Ltd (Chengdu, China), with purity all ≥98%. Caffeic acid (No. M28HB183194) was acquired from Shanghai Yuanye Biotechnology Co., Ltd (Shanghai, China), with purity ≥98%. Acetonitrile was purchased from Sigma-Aldrich Trading Co., Ltd (Shanghai, China). Phosphoric acid was sourced from Tianjin Kermel Chemical Reagent Co., Ltd (Tianjin, China). Ethanol was provided by Sinopharm Chemical Reagent Co., Ltd (Shanghai, China).

A total of 17 batches of CA were collected from different provinces in China, including Southwest China (Sichuan, Guizhou, Chongqing), East China (Anhui, Zhejiang, Shandong), Central China (Henan, Hubei, Hunan), and Hebei Province. Detailed information regarding their origins, latitude, longitude, and altitude is provided in Table 1. All samples were verified as the dried whole herb of *Carpesium abrotanoides* L. by Prof. Wang Zhi from Hunan University of Chinese Medicine.

2.2 Preparation of solutions

2.2.1 Preparation of sample solutions. The CA medicinal materials were pulverized and filtered using a 60-mesh sieve. 0.5 g of CA powder was accurately weighed, and 50 mL of 80% ethanol was accurately added. Ultrasonic extraction (200 W, 40 kHz) was performed for 60 minutes. Upon cooling, 80% ethanol was added to compensate for the loss in weight. The sample was filtered through a 0.22 μm organic microporous membrane to acquire the test solution. The extraction solvent (80% ethanol) was filtered through the same microporous membrane to serve as the blank solution.

2.2.2 Preparation of standard solutions. Appropriate amounts of the reference standard, namely chlorogenic acid,

 © 2026 The Author(s). Published by the Royal Society of Chemistry

Open Access Article. Published on 13 February 2026. Downloaded on 5/20/2026 7:02:52 PM. This article is licensed under a Creative Commons Attribution-NonCommercial 3.0 Unported Licence.

Table 1 The similarities of CA from different origins

CA	Origins	Latitude and longitude	Altitude/m	Similarity
S1	Bozhou, Anhui	115°45′08.1″E, 33°52′49.4″N	41	0.922
S2	Bozhou, Anhui	115°44′03.0″E, 33°53′03.7″N	42	0.965
S3	Bozhou, Anhui	115°44′29.8″E, 33°53′08.6″N	38	0.950
S4	Meishan, Sichuan	103°51′56.6″E, 30°04′52.3″N	416	0.967
S5	Guangan, Sichuan	106°38′17.2″E, 30°26′30.9″N	298	0.977
S6	Nanyang, Henan	112°30′29.2″E, 33°02′45.6″N	123	0.988
S7	Nanyang, Henan	112°27′51.0″E, 33°02′32.2″N	123	0.949
S8	Pingdingshan, Henan	113°14′47.2″E, 33°47′37.8″N	221	0.881
S9	Shiyan, Hubei	110°51′22.9″E, 32°39′50.9″N	341	0.870
S10	Zunyi, Guizhou	106°55′34.0″E, 27°43′43.0″N	881	0.906
S11	Bijie, Guizhou	105°20′44.7″E, 27°18′30.4″N	1500	0.694
S12	Liangping, Chongqing	107°48′34.3″E, 30°40′38.4″N	482	0.982
S13	Jining, Shandong	116°34′42.5″E, 35°33′35.5″N	38	0.905
S14	Baoding, Hebei	115°19′50.0″E, 38°51′09.2″N	22	0.893
S15	Xianju, Zhejiang	120°41′57.1″E, 28°51′07.6″N	9	0.928
S16	Hangzhou, Zhejiang	120°06′44.2″E, 30°14′04.2″N	52	0.985
S17	Jishou, Hunan	109°41′38.4″E, 28°16′02.6″N	188	0.950

caffeic acid, cynaroside, 11(13)-dehydroivaxillin, isochlorogenic acid A, isochlorogenic acid C, 2,3,4,5-tetracaffeoyl-D-glucaric acid, 2-deoxy-4-*epi*-gaillardin, carabrone, and telekin, were accurately weighed and dissolved in 80% ethanol to prepare stock solutions with a certain mass concentration for the single reference standard. The mixed reference standard stock solutions with mass concentrations of 158.88, 19.86, 149.76, 95.70, 445.20, 19.96, 72.94, 173.50, 63.84, and 67.50 μg mL^{-1} were prepared by mixing and diluting appropriate amounts of the single reference standard stock solutions.

2.3 UPLC chromatographic condition

Experimental analyses were carried out on the Waters Acquity UPLC H-Class liquid chromatography system that is equipped with an autosampler manager, a PDA detector, and a quaternary solvent delivery pump (Waters, MA, USA). The Waters ACQUITY UPLC ® BEH C_{18} chromatographic column (2.1 × 100 mm, 1.7 μm) was employed to separate the samples at 35 °C. The mobile phase consisted of 0.1% phosphoric acid (A) and acetonitrile (B), with gradient elution of 10% B (0–2 min), 10–14.5% B (2–5 min), 14.5–22% B (5–15 min), 22–26% B (15–17 min), 26–28% B (17–25 min), 28–37% B (25–30 min) at a flow rate of 0.3 mL min^{-1}. The detection wavelength was set at 230 nm, and the injection volume was 0.5 μL for the UPLC analysis.

2.4 Identification of common peaks by UPLC-Q-TOF-MS

The UPLC-Q-TOF-MS analysis was performed on a Waters Acquity H-class UPLC system coupled with a Xevo G2-XS-Q-TOF mass spectrometer (Waters, MA, USA), with data acquisition and processing were controlled by Masslynx 4.2 software. The UPLC chromatographic conditions were consistent with those described above, except that the mobile phase A was replaced with 0.1% formic acid in water. The mass spectrometer was operated with electrospray ionization (ESI) using rapid polarity switching to acquire data in both positive (ESI^+) and negative (ESI^-) modes simultaneously. The source parameters were set as follows: capillary voltage was set to 3 kVfor ESI^+ and 2.5 kV for ESI^-, cone voltage 30 V, ion source temperature 120 °C, desolvation temperature 400 °C, and desolvation gas flow rate 800 L h^{-1} acquired using MS^E mode over a 30-minute runtime with a mass range of 100–1500 Da. Collision energy was set at 20–50 V with high-purity argon as the collision gas. Leucineenkephalin was used for real-time mass calibration.

Based on literature reports, chemical component information related to CA was collected to establish a component database. The database and LC-MS raw data were imported into UNIFI software (Waters, MA, USA) for component matching. 19 common peaks were identified by combining online databases PubChem (https://pubchem.ncbi.nlm.nih.gov) and ChemSpider (https://www.chemspider.com), along with literature-reported fragmentation rules of compounds and fragmentation rules of reference standards.

2.5 Fingerprint similarity and chemometric analysis

The Chinese Medicine Chromatographic Fingerprint Similarity Evaluation System (Version 2012) was employed to evaluate sample similarity by inputting the chromatogram data from S1 to S17 into the software. Isochlorogenic acid A was selected as the reference peak (S) owing to its comparatively large peak area and moderate retention period. Multi-point correction was executed utilising the average method, with the time window width established at 0.1 min. A reference fingerprint was generated, and the similarity coefficient of each sample relative to this reference fingerprint was calculated by employing the cosine similarity method.

A correlation heatmap was generated using Origin Pro 2021 software to visualize the inter-batch correlations based on the peak areas of the 19 common peaks. In addition, the same data matrix was subjected to further chemometric analyses. Hierarchical clustering analysis (HCA) was performed using TBtools software based on the Euclidean squared distance. Principal component analysis (PCA), and orthogonal partial least squares-discriminant analysis (OPLS-DA) using SIMCA 14.1, and

Open Access Article. Published on 13 February 2026. Downloaded on 5/20/2026 7:02:52 PM. This article is licensed under a Creative Commons Attribution-NonCommercial 3.0 Unported Licence.

MetaboAnalyst 6.0 software to identify potential chemical markers responsible for quality differences.

2.6 Method validation

0.25, 0.50, 1.00, and 2.00 mL of the mixed reference standard stock solution were precisely pipetted, and the volume was made up to 5 mL with 80% ethanol, respectively, to prepare 5 mixed reference standard solutions at varying concentrations. The mixed standards at different concentrations (x) were injected, and the corresponding peak areas (y) of the analytes were quantified to generate standard curves. The LOD and LOQ were defined as signal-to-noise ratios (S/N) of 3 and 10, respectively. According to the liquid phase method, injection was performed to determine the RSD values of precision, repeatability, and stability. The mixed standard solutions containing equal amounts of each component were spiked into a 0.25 g sample (S17). The spiked samples were prepared following the sample preparation method, with 6 replicates. 6 mixed samples were injected for analysis, and the RSDs of each component were calculated to validate the study accuracy.

2.7 QAMS analysis

2.7.1 Calculation of RCFs. Using isochlorogenic acid A as the internal standard, the relative correction factors (RCFs) for chlorogenic acid, caffeic acid, cynaroside, 11(13)-dehydroivaxillin, isochlorogenic acid C, 2,3,4,5-tetracaffeoyl-D-glucaric acid, 2-deoxy-4-*epi*-gaillardin, carabrone, and telekin were calculated using 5 different concentration levels mixed reference standard solutions to ensure accuracy. At each level, samples were analyzed in triplicate. The calculation was performed using the following equation RCF $= (A_s/C_s)/(A_i/C_i)$. Where C_s and C_i refer to the concentrations of the internal standard substance and the components to be measured, and A_s and A_i stand for the peak areas of the internal standard and the components to be measured, respectively.

2.7.2 System suitability test and chromatographic peak localization. The impacts of different brands of UPLC system (Waters H-class, Agilent Infinity II, and Thermo scientific U3000), chromatographic columns (Waters, Agilent, and Thermo scientific), distinct flow rates (0.2, 0.3, 0.4 mL min^{-1}), and varying column temperatures (33, 35, 37 °C) on the relative correction factors were also examined and evaluated. The relative retention time ($R_t = t_i/t_s$) was used to locate the chromatographic peaks. In this context, R_t means the ratio of the retention time, t_i denotes the retention time of each analyte to be measured, and t_s signifies the retention time of the internal standard (isochlorogenic acid A).

2.7.3 Content determination of samples and quality fluctuation analysis. The contents of 10 components in 17 batches of CA samples were determined by the QAMS and ESM (external standard method), respectively. Triplicate samples were prepared for each batch, and the relative error (RE) between the two methods was calculated as per the equation: RE (%) = (QAMS − ESM)/ESM × 100.

During quantitative analysis, parameter P was employed and computed to determine the quality fluctuation performance of samples according to the formula $P = C_i/\acute{C}_i$, where C_i denotes the measured concentration of a certain component, and $\acute{C}_i$ signifies the average concentration of 17 batches of CA.

3 Results and discussion

3.1 Optimization of chromatographic conditions

Due to the complex composition of CA, it is exceedingly challenging to achieve their separation *via* a straightforward isocratic elution method. Therefore, it is crucial to systematically optimize chromatographic conditions for analyzing complex plant chemical components. In preliminary method optimization, the UPLC system was refined for different mobile phases (acetonitrile–water, acetonitrile–0.1% phosphoric acid in water, and methanol–0.1% phosphoric acid in water). Column types (C_{18} and T_3) and column temperatures (33 °C, 35 °C, and 37 °C) were examined and optimized. A Photodiode Array (PDA) detector was configured to carry out 3D full-wavelength scanning across the spectrum of 190–400 nm. Ultimately, given the peak elution order, resolution, number of chromatographic peaks, and peak shape of the samples, the preferred conditions were a Waters ACQUITY UPLC ® BEH C_{18} column (2.1 × 100 mm, 1.7 μm) with acetonitrile water containing 0.1% phosphoric acid as the mobile phase at a flow rate of 0.3 mL min^{-1}, and a column temperature of 35 °C. An amount of 0.5 μL was injected. The representative UPLC chromatograms of the blank solution, mixed standard solution, and CA sample were depicted in Fig. 1B. Under the optimal chromatographic conditions, all analytes were effectively separated at appropriate retention durations.

3.2 Fingerprint establishment and common peaks identification

The fingerprints of CA for different batches were illustrated in Fig. 1A and B. It could be seen that the fingerprints comprise 19 common peaks in total. To elucidate the chemical basis of this fingerprint, the components corresponding to these 19 common peaks were identified by UPLC-Q-TOF-MS. The detailed identification results were shown in Table 2, which indicated that a total of 6 sesquiterpene components, 11 phenolic acid components, and 2 flavonoid components were identified from 19 common peaks. Among these, peaks 1, 2, 7, 9, 10, 12, 13, 15, 16, and 17 were specifically identified by comparison with reference standards as chlorogenic acid, caffeic acid, cynaroside, 11(13)-dehydroivaxillin, isochlorogenic acid A, isochlorogenic acid C, 2,3,4,5-tetracaffeoyl-D-glucaric acid, 2-deoxy-4-*epi*-gaillardin, carabrone, and telekin. The structures of the aforementioned components were shown in Fig. 1C, providing a robust foundation for the subsequent quality evaluation.

3.3 Similarity analysis and correlation analysis

3.3.1 Similarity analysis. To evaluate the overall quality consistency among 17 batches, a similarity analysis was performed using The Chinese Medicine Chromatographic Fingerprint Similarity Evaluation System (Version 2012). As shown in

 © 2026 The Author(s). Published by the Royal Society of Chemistry

Open Access Article. Published on 13 February 2026. Downloaded on 5/20/2026 7:02:52 PM.
This article is licensed under a Creative Commons Attribution-NonCommercial 3.0 Unported Licence.

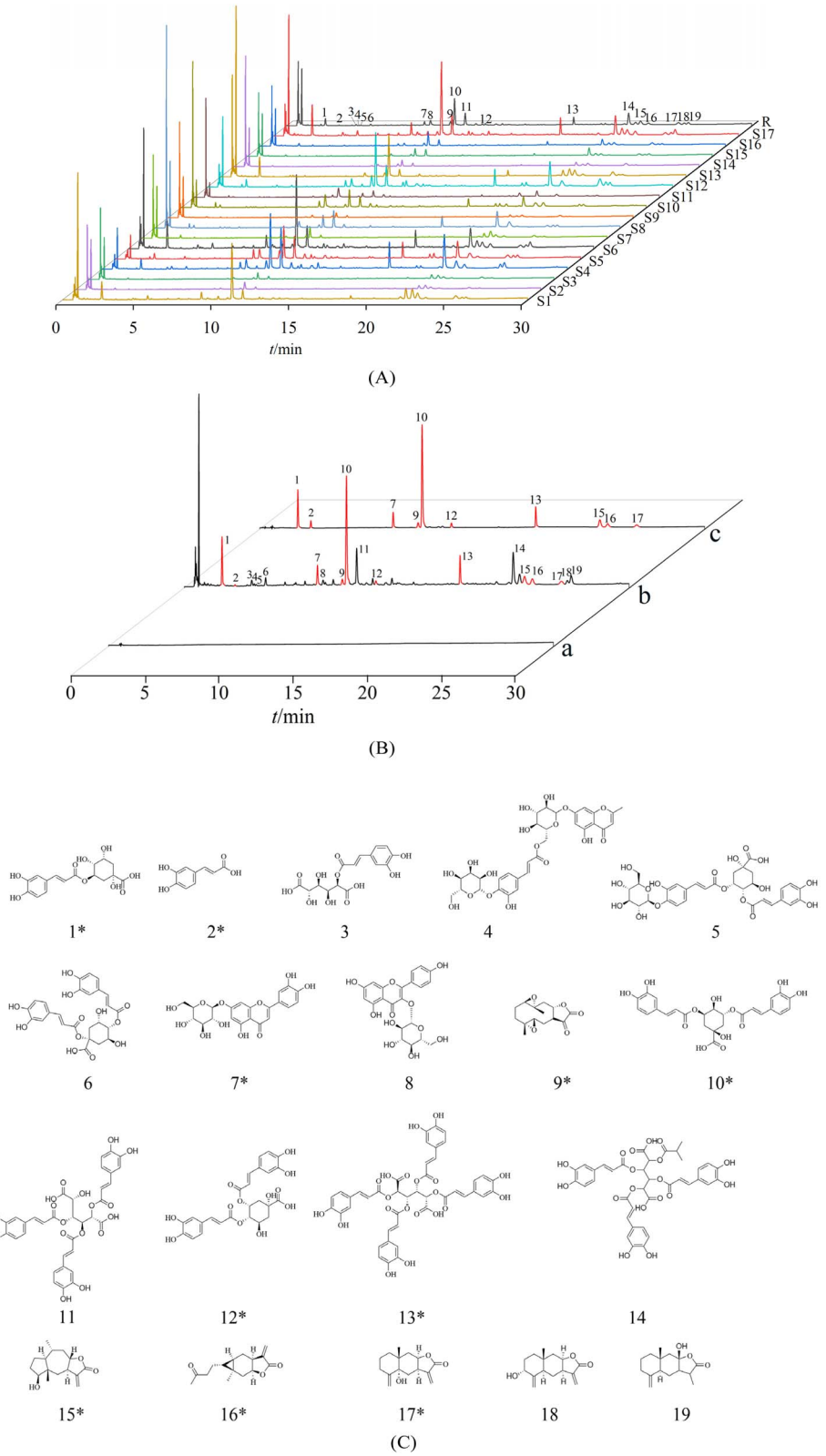

Fig. 1 (A) The fingerprints of CA for different origins. (B) UPLC chromatograms (a: blank-80% ethanol; b: sample; c: mixed standards). (C) Structures of the 19 common components. *Representing quantitative components.

Table 1, the similarity coefficients ranged from 0.694 to 0.988 and the majority of samples (16 out of 17) exhibited high similarity (>0.880). This indicates a general consistency in the chemical profiles across different batches, suggesting that the established UPLC fingerprint may be employed in evaluating the quality of CA.

Open Access Article. Published on 13 February 2026. Downloaded on 5/20/2026 7:02:52 PM.
This article is licensed under a Creative Commons Attribution-NonCommercial 3.0 Unported Licence.

Table 2 Identification of common peaks in CA

No.	RT(min)	Identification	Formula	Reference ion	*m/z*	Diff. (ppm)	Fragmentations (*m/z*)	Classification	References
1[a]	2.521	Chlorogenic acid	$C_{16}H_{18}O_9$	$[M-H]^-$	353.0874	0.3	191.0552, 135.0442	Phenolic acid	33 and 34
2[a]	3.408	Caffeic acid	$C_9H_8O_4$	$[M-H]^-$	179.0343	−0.6	161.0419, 135.0444, 121.0313	Phenolic acid	34
3	4.502	2-*O*-Caffeoylglucaric acid	$C_{31}H_{34}O_{17}$	$[M-H]^-$	371.0678	1.3	191.0551, 179.0346, 153.0902, 135.0412	Phenolic acid	PubChem, Chemspider
4	4.679	5-Hydroxy-2-methyl-4-oxo-4*H*-chromen-7-yl 6-*O*-{(2*E*)-3-[4-(β-D-allopyranosyloxy)-3-hydroxyphenyl]-2-propenoyl}-β-D-glucopyranoside	$C_{31}H_{34}O_{17}$	$[M-H]^-$	677.1714	−0.6	191.0546, 179.0543, 161.0435, 135.044 8	Phenolic acid	PubChem, Chemspider
5	4.805	(1*R*,3*R*,4*S*,5*R*)-4-{[(2*E*)-3-(3,4-Dihydroxyphenyl)-2-propenoyl]oxy}-3-({(2*E*)-3-[4-(β-acetonitrile-water-glucopyranosyloxy)-3-hydroxyphenyl]-2-propenoyl}oxy)-1,5-dihydroxycyclohexanecarboxylic acid	$C_{31}H_{34}O_{17}$	$[M-H]^-$	677.1714	−0.6	515.1121, 353.0899, 191.0543, 179.0349, 161.0248, 135.0441	Phenolic acid	PubChem, Chemspider
6	5.442	Cynarin	$C_{25}H_{24}O_{12}$	$[M-H]^-$	515.1188	−0.4	353.0872, 335.0752, 191.0549, 179.0339, 161.0231,135.0440	Phenolic acid	34
7*	8.925	Cynaroside	$C_{21}H_{20}O_{11}$	$[M+H]^+$	449.1080	−0.9	287.0551, 269.0435, 241.0490, 153.0186, 135.0440	Flavonoid	35
8	9.322	Astragalin	$C_{21}H_{20}O_{11}$	$[M-H]^-$	447.0928	0.2	285.0392, 151.0023	Flavonoid	36
9[a]	10.600	11(13)-Dehydroivaxillin	$C_{15}H_{20}O_4$	$[M+H]^+$	265.1441	0.4	247.1326, 229.1224, 201.1280	Sesquiterpene	4
10[a]	10.871	Isochlorogenic acid A	$C_{25}H_{24}O_{12}$	$[M-H]^-$	515.1190	0.0	353.0870, 335.0763, 191.0553, 179.0337, 173.0445, 135.0441	Phenolic acid	37
11	11.557	Leontopodic acid B	$C_{33}H_{28}O_{17}$	$[M-H]^-$	695.1247	−0.1	533.0927, 371.0612, 209.0290, 191.0186, 179.0339, 161.0230	Phenolic acid	38
12[a]	12.841	Isochlorogenic acid C	$C_{25}H_{24}O_{12}$	$[M-H]^-$	515.1193	0.6	353.0874, 191.0547, 173.0443, 135.0464	Phenolic acid	37
13[a]	18.531	2,3,4,5-Tetracaffeoyl-D-glucaric acid	$C_{42}H_{34}O_{20}$	$[M-H]^-$	857.1567	0.2	695.1256, 533.0934, 371.0613, 209.0291, 191.0187, 179.0337, 161.0235, 133.0280, 116.9273	Phenolic acid	PubChem, Chemspider
14	22.080	2,3,4-Tris[[(*E*)-3-(3,4-dihydroxyphenyl) prop-2-enoyl]oxy]-5-(2-methylpropanoyloxy)hexanedioic acid	$C_{37}H_{33}O_{18}$	$[M-H]^-$	765.1666	−0.1	603.1354, 441.1035, 279.0713, 191.0185, 179.0337, 161.0229, 135.0437	Phenolic acid	PubChem, Chemspider
15[a]	22.854	2-Deoxy-4-*epi*-gaillardin	$C_{15}H_{22}O_3$	$[M+H]^+$	251.1642	−1.7	233.1531, 215.1429, 187.1482, 115.0547	Sesquiterpene	39
16[a]	23.361	Carabrone	$C_{15}H_{20}O_3$	$[M+H]^+$	249.1489	−0.8	231.1384, 213.1270, 203.1428, 185.1332, 157.1010	Sesquiterpene	40
17[a]	25.311	Telekin	$C_{15}H_{20}O_3$	$[M+H]^+$	249.1494	−2.1	231.1364, 213.1270, 203.1427, 185.1325	Sesquiterpene	41
18	25.678	Isotelekin	$C_{15}H_{20}O_3$	$[M+H]^+$	249.1491	0.0	231.1364, 185.1332	Sesquiterpene	42
19	25.940	Atractylenolide III	$C_{15}H_{20}O_3$	$[M+H]^+$	249.1493	0.8	185.1363	Sesquiterpene	42

[a] Identified by comparison with reference standard.

© 2026 The Author(s). Published by the Royal Society of Chemistry

Open Access Article. Published on 13 February 2026. Downloaded on 5/20/2026 7:02:52 PM.
This article is licensed under a Creative Commons Attribution-NonCommercial 3.0 Unported Licence.

The similarity among batches varies, which may be related to geographical factors. A trend was observed where samples form subtropical monsoon climate regions (Southwest, East, and Central China) showed higher similarity (mostly ≥0.900), likely due to favorable hydrothermal conditions. In contrast, sample from temperate monsoon climates, such as S14 (form Baoding, Hebei), S8 (form Pingdingshan, Henan) displayed lower similarity. Furthermor e, landform and soil type appeared to amplify these differences. For instance, S11 sourced form the karst plateau of Guizhou with thin soil layers and high nutrient loss, resulting in a relatively low similarity of only 0.694.[43,44] Similarly, S9 originated from Hubei, where karst landform corrosion has led to generally thin soil layers with poor water and fertilizer retention capacity, displayed a comparatively low similarity score.[45]

3.3.2 Inter-batch correlation analysis. While similarity analysis compares each sample to the reference fingerprint, it does not directly reveal the relationships between individual batches. To address this, 19 common peak areas were input as variables into Origin Pro 2021 software, and a correlation heatmap was generated (Fig. 2). The analysis provided a more nuanced view of inter-batch variations. For example, the correlation coefficient between samples S15 and S16, both from Zhejiang Province, reached as high as 0.96. S11 showed low correlation with other samples, which further explained its similarity of only 0.694. Notably, the analysis also revealed variations even within the same origin, such as the low correlation (0.76) between S1 and S2, both form Bozhou, Anhui.

Collectively, the combination of similarity and correlation analyses effectively assessed the overall consistency and highlighted differences among the CA batches. However, these fingerprint-based methods are primarily qualitative or semi-quantitative. They reveal that differences exist but do not pinpoint the potential components of these variations, nor do they provide accurate quantitative data for quality control. Therefore, to develop a more comprehensive and systematic evaluation strategy, it was necessary to adopt chemometric analysis and established a reliable quantitative method.

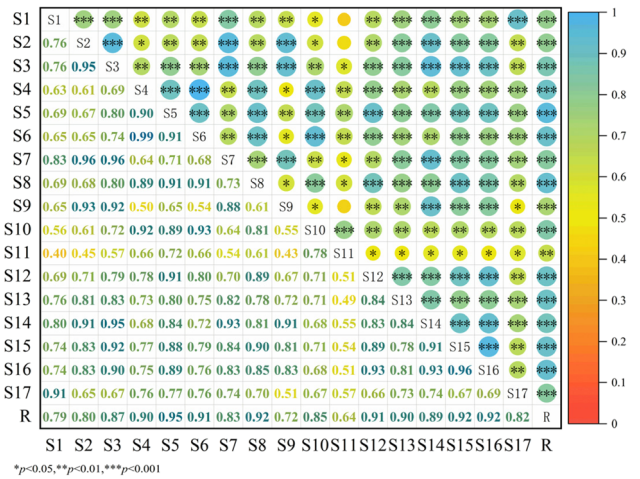

Fig. 2 Correlation heat map of 17 batches of samples.

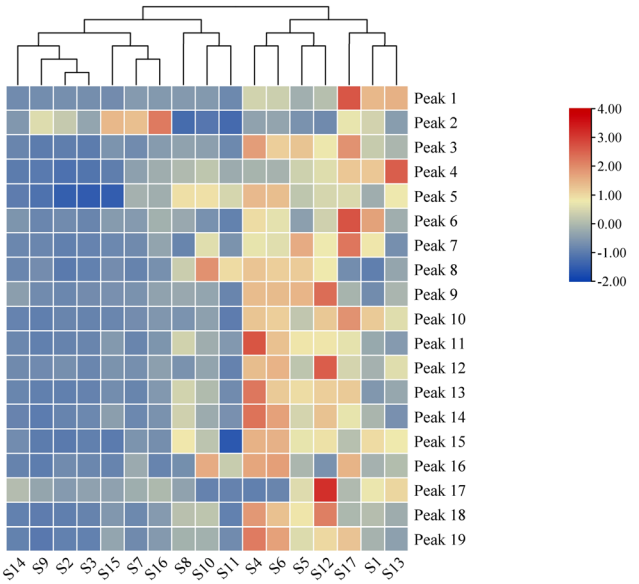

Fig. 3 HCA heat map of 17 batches of CA.

3.4 Chemometric analysis

3.4.1 Hierarchical cluster analysis. HCA constructs dendrograms by quantifying pairwise similarities through the squared Euclidean distance metric, hence generating nested cluster hierarchies based on sample dissimilarity.[46] The result of the heat map was presented in Fig. 3. The scale bar in the figure represents the *Z*-score normalized peak areas, where the gradient form blue (low) to red (high) indicates the relative abundance of each component in a given sample compared to its average abundance across all sample. The 17 batches of CA samples were categorized into 2 clusters: one consisting of S1, S4, S5, S6, S12, S13, and S17 and the other comprising S2, S3, S7, S8, S9, S10, S11, S14, S15, and S16. The results highlighted that chemical compositions differences existed in 17 batches of CA samples, and the classification was related to the content levels of the constituents. Samples from the same province tended to cluster together, with the exception of those from Anhui and Henan provinces, which showed some overlap. This may be related to factors such as the harvest time and storage conditions. Therefore, the production areas of CA medicinal materials cannot fully reflect their quality, and the content of their chemical compositions should also be considered comprehensively.

3.4.2 Principal component analysis. As an unsupervised method for dimensionality reduction, PCA reduces correlated variables to orthogonal principal components that retain the maximal variance.[47] The score plot (Fig. 4A) showed that two primary components were obtained, exhibiting variance contributions of 62.2% and 13.7%, respectively. This indicated that the extracted principal components thoroughly characterized the chemical information of the medicinal materials. The PCA scatter plot intuitively showed the differences and similarities among the samples. Notably, the sample distribution in the PCA plot corresponded with the HCA findings, providing a foundation for the subsequent supervised analysis to identify discriminant compounds.

Open Access Article. Published on 13 February 2026. Downloaded on 5/20/2026 7:02:52 PM.
This article is licensed under a Creative Commons Attribution-NonCommercial 3.0 Unported Licence.

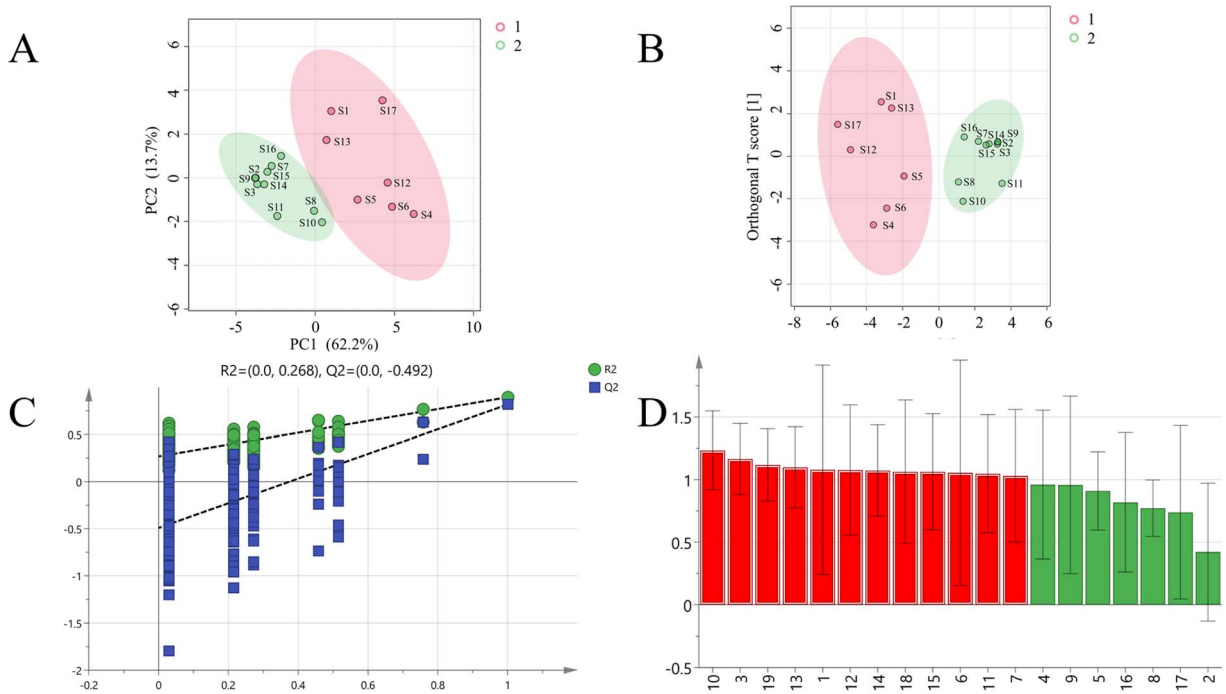

Fig. 4 (A) PCA of Carpesium abrotanoides from different origins. (B) OPLS-DA. (C) Permutation test results of the OPLS-DA model. (D) VIP values for 19 common peaks in the OPLS-DA model.

3.4.3 Orthogonal partial least squares-discriminant analysis. To further analyze the differences between the two identified groups, OPLS-DA was applied to profile metabolic disparities, using VIP >1.0 as the threshold for identifying discriminatory markers.[48] The OPLS-DA result was presented in Fig. 4B. The model parameters were $R^2X = 0.752$, $R^2Y = 0.894$, and $Q^2 = 0.817$. Both R^2 and Q^2 exceeded 0.5, confirming the model's reliability. Perform permutation 200 times for the OPLS-DA model to generate the permutation test plot (Fig. 4C). The findings indicated that the intercepts of R^2 and Q^2 on the *Y*-axis were both inferior to the original values, meaning that the established model was not overfitted.

The VIP score plot (Fig. 4D) showed that the VIP values of peaks 10, 3, 19, 13, 1, 12, 14, 18, 15, 6, 11, and 7 were 1.2334, 1.1649, 1.1174, 1.0983, 1.0790, 1.0735, 1.0767, 1.0735, 1.0633, 1.0631, 1.0547, and 1.0474, respectively. Their VIP values were all greater than 1. The 12 components contributed significantly to the observed chemical variations among samples from different regions, suggesting a possible influence of geographical origin, and could be regarded as potential differential components of CA. Among them, peaks 10, 13, 1, 12, 15, and 7 were designated as isochlorogenic acid A, 2,3,4,5-tetracaffeoyl-D-glucaric acid, chlorogenic acid, isochlorogenic acid C, 2-deoxy-4-*epi*-gaillardin, and cynaroside, respectively.

3.5 Validation of UPLC methods

3.5.1 Investigation of linear range, LOD, and LOQ. 10 components, namely chlorogenic acid (1), caffeic acid (2), cynaroside (3), 11(13)-dehydroivaxillin (4), isochlorogenic acid A (5), isochlorogenic acid C (6), 2,3,4,5-tetracaffeoyl-D-glucaric acid (7), 2-deoxy-4-*epi*-gaillardin (8), carabrone (9), and telekin (10), were utilized as markers for linear range evaluation. The evaluation was conducted by formulating reference standard solutions at varying concentrations and building regression equations *via* the least squares method. The limit of detection (LOD) and limit of quantification (LOQ) for each component were determined at a signal-to-noise (S/N) ratio of 3 and 10, respectively. Table 3 showed that the correlation coefficients (r^2) for all components were above 0.9995, implying that within the observed concentration range, the analyzed components exhibited strong linear correlations between concentrations and peak areas.

3.5.2 Investigation of precision, stability, repeatability, and recovery. All the results pertaining to the precision, stability, repeatability and recovery were enumerated in Table 3. Precision assessment revealed that the relative standard deviation (RSD) values for each index component ranged from 0.53% to 2.43%, signifying that the method boasts exceptional precision. The stability test further indicated that the RSDs values were between 0.79% and 2.07%, attesting that the CA sample solutions remained stable within 24 hours. The repeatability analysis showed that the RSDs values were below 3%, manifesting the favorable repeatability of this method.

As reported in Table 3, the average recoveries of 10 components were 98.71%, 102.26%, 101.47%, 98.12%, 99.43%, 94.65%, 95.48%, 103.06%, 97.57%, and 98.84% respectively, and the RSDs were all below 2.79%. The results affirmed the high accuracy of this method.

3.6 Establishment of QAMS method

3.6.1 Calculation of RCFs. The RCFs for each analyte was calculated to enable quantification using only the internal

© 2026 The Author(s). Published by the Royal Society of Chemistry

Open Access Article. Published on 13 February 2026. Downloaded on 5/20/2026 7:02:52 PM. This article is licensed under a Creative Commons Attribution-NonCommercial 3.0 Unported Licence.

Table 3 Results of linear ranges, LOD, LOQ, RSD values (%) for precision, stability, reproducibility, and spiked recoveries of the ten standards (n = 6)

Components	Standard curves	(r^2)	Linear ranges (μg mL^{-1})	LOD (μg mL^{-1})	LOQ (μg mL^{-1})	Precision (RSD/%)	Stability (RSD/%)	Repeatability (RSD/%)	Spiked recovery (%)	Spiked recovery (RSD/%)
Component 1	$y = 2770.2x - 14446$	0.9998	7.94–158.88	0.40	0.79	0.53	1.02	1.69	98.71	2.55
Component 2	$y = 4715.7x - 3513.6$	0.9997	0.99–19.86	0.10	0.99	1.78	1.03	2.75	102.26	2.61
Component 3	$y = 1446.4x - 7604.7$	0.9998	7.49–149.76	0.10	3.00	0.91	1.45	2.55	101.47	1.47
Component 4	$y = 1024.3x - 2904.8$	0.9995	4.79–95.70	0.96	4.79	2.00	1.70	2.22	98.12	0.79
Component 5	$y = 3620.1x - 43786$	0.9997	22.26–445.20	0.22	1.11	0.58	0.80	1.52	99.43	1.01
Component 6	$y = 3705.2x - 2754.8$	0.9997	1.00–19.96	0.20	1.00	0.69	0.79	2.01	94.65	1.18
Component 7	$y = 3831.6x - 8960.2$	0.9995	3.65–72.94	0.18	0.73	2.43	0.99	2.61	95.48	1.67
Component 8	$y = 1269.9x - 6287.3$	0.9997	8.68–173.50	1.74	3.47	1.00	1.13	0.63	103.06	0.69
Component 9	$y = 1801.2x - 3318.5$	0.9995	3.19–63.84	1.28	3.19	1.10	0.77	0.98	97.57	2.15
Component 10	$y = 1205.9x - 1994.9$	0.9997	3.38–67.50	1.35	3.38	2.15	2.07	2.37	98.84	2.79

standard. In the present study, component 5 served as an internal standard for its superior separation performance, moderate retention value, and low cost. The results of RCFs for the other 9 components were listed in Table 4. The RCFs for components 1, 2, 3, 4, 6, 7, 8, 9, and 10 were 1.32, 0.79, 2.55, 3.60, 1.00, 0.98, 2.88, 2.01 and 3.09, with RSD values of 0.87%, 1.76%, 1.06%, 1.90%, 1.72%, 2.85%, 2.97%, 2.82% and 2.00%, respectively. The precision of these RCFs was excellent, confirming the stability of the measurements.

3.6.2 System suitability test. To rigorously assess the durability and practical applicability of the method, the robustness of the RCFs was evaluated under a wide range of chromatographic variations. This comprehensive test included using three different brands of UPLC system (Waters, Agilent, and Thermo Scientific), six different columns form three manufacturers (Waters, Agilent, and Thermo Scientific), varying flow rates (0.2, 0.3, 0.4 mL min^{-1}), and different column temperatures (33, 35, 37 °C). As shown in Tables S1, the RSDs of the relative correction factors of all index components under different conditions were less than 3.99%, indicating that these parameters did not exert significant influence on RCFs and the QAMS method exhibited robust durability under diverse conditions.

3.6.3 Location of chromatographic peaks of analytes to be measured. The relative retention time (R_t) between the internal reference and the component was calculated to localize the peak of the component to be tested. The RSDs of the relative retention times of all analyte were under 3.11% (Table S2), indicating that there were little fluctuations across different instruments, columns, flow rates, and column temperatures. This R_t has good reproducibility and can be used to localize peaks for the other nine components in the CA.

3.6.4 Content determination of samples. The results of the contents of the above 10 components determined by QAMS and ESM were enumerated in Table 5. It is apparent that RE values fell within ±2.0%, indicating no substantial variations between the ESM and QAMS methods. The results demonstrated that it was feasible to simultaneously determine 10 components in CA using QAMS. The average contents of components 1–10 were 0.38, 0.34, 0.40, 0.79, 1.27, 0.07, 0.30, 1.10, 0.28, and 0.70 mg g^{-1}, respectively.

According to Fig. 5, the content of components of different batches of CA varies significantly, and the contents of component 5 and component 8 were relatively high in the majority of samples. The total content of the 10 components showed

Table 4 The RCFs of component (n = 3)

Level	Component 1	Component 2	Component 3	Component 4	Component 6	Component 7	Component 8	Component 9	Component 10
Level 1	1.34	0.78	2.52	3.71	1.02	1.00	3.03	1.91	3.07
Level 2	1.32	0.81	2.59	3.61	1.03	1.01	2.82	2.02	3.17
Level 3	1.31	0.78	2.54	3.58	1.00	0.97	2.87	2.05	3.10
Level 4	1.32	0.79	2.55	3.54	0.99	0.96	2.85	2.05	3.09
Level 5	1.31	0.77	2.53	3.56	0.99	0.95	2.84	2.00	3.00
Means	1.32	0.79	2.55	3.60	1.00	0.98	2.88	2.01	3.09
RSD,%	0.87	1.76	1.06	1.90	1.72	2.85	2.97	2.82	2.00

Open Access Article. Published on 13 February 2026. Downloaded on 5/20/2026 7:02:52 PM. This article is licensed under a Creative Commons Attribution-NonCommercial 3.0 Unported Licence.

Table 5 QAMS and ESM determination of ten components in 17 batches of CA (mg g^{-1}, $n = 3$)[a]

Components	Method	S1	S2	S3	S4	S5	S6	S7	S8	S9	S10	S11	S12	S13	S14	S15	S16	S17
Component 5	ESM	2.63	0.33	0.28	2.68	1.53	2.56	0.47	0.57	0.20	0.06	0.18	2.65	1.95	0.27	0.34	0.64	3.42
Component 1	ESM	0.95	0.10	0.10	0.55	0.31	0.52	0.18	0.17	0.09	0.17	0.06	0.42	0.99	0.08	0.09	0.17	1.45
	QAMS	0.96	0.10	0.10	0.55	0.32	0.53	0.18	0.17	0.09	0.17	0.06	0.42	1.00	0.08	0.09	0.17	1.46
	RE/%	0.71	1.01	1.14	0.78	0.69	0.81	0.92	0.99	1.22	0.93	1.04	0.84	0.70	0.76	1.30	0.78	0.68
Component 2	ESM	0.03	0.03	N/A	N/A	N/A	N/A	0.04	N/A	0.03	N/A	N/A	N/A	N/A	N/A	0.04	0.05	0.03
	QAMS	0.03	0.03	N/A	N/A	N/A	N/A	0.04	N/A	0.03	N/A	N/A	N/A	N/A	N/A	0.04	0.05	0.03
	RE/%	0.77	3.96	N/A	N/A	N/A	N/A	1.70	N/A	2.93	N/A	N/A	N/A	N/A	N/A	1.85	2.40	0.44
Component 3	ESM	0.75	N/A	N/A	0.69	1.03	0.66	0.14	N/A	N/A	0.66	0.20	0.73	0.17	0.12	0.13	0.30	1.29
	QAMS	0.75	N/A	N/A	0.70	1.03	0.66	0.14	N/A	N/A	0.66	0.20	0.73	0.17	0.12	0.13	0.30	1.29
	RE/%	0.28	N/A	N/A	0.17	0.21	0.16	0.67	N/A	N/A	0.29	0.23	0.16	0.58	0.17	0.35	0.42	0.21
Component 4	ESM	0.29	0.24	0.30	1.74	1.80	1.75	0.36	0.61	0.28	0.57	0.22	2.45	0.75	0.50	0.35	0.54	0.74
	QAMS	0.30	0.24	0.30	1.75	1.81	1.76	0.36	0.61	0.28	0.58	0.22	2.46	0.75	0.50	0.35	0.54	0.74
	RE/%	0.69	0.81	0.74	0.55	0.51	0.54	0.76	0.52	0.78	0.54	0.81	0.51	0.58	0.64	0.57	0.60	0.51
Component 6	ESM	0.07	N/A	N/A	0.20	0.10	0.21	N/A	N/A	N/A	0.05	N/A	0.30	0.13	N/A	N/A	0.04	0.12
	QAMS	0.07	N/A	N/A	0.20	0.10	0.21	N/A	N/A	N/A	0.05	N/A	0.30	0.13	N/A	N/A	0.04	0.12
	RE/%	1.57	N/A	N/A	0.59	1.44	0.60	N/A	N/A	N/A	1.44	N/A	0.47	0.90	N/A	N/A	1.12	0.48
Component 7	ESM	0.13	N/A	N/A	1.00	0.60	0.67	0.03	0.43	N/A	0.31	0.06	0.66	0.21	0.04	0.07	0.13	0.68
	QAMS	0.13	N/A	N/A	1.01	0.61	0.68	0.03	0.44	N/A	0.31	0.07	0.67	0.21	0.04	0.08	0.13	0.68
	RE/%	0.99	N/A	N/A	0.97	0.93	0.91	1.72	0.93	N/A	1.11	1.92	0.98	0.93	1.05	1.93	1.61	0.99
Component 8	ESM	1.76	0.42	0.49	2.10	1.57	2.11	0.71	1.65	0.45	1.22	N/A	1.71	1.63	0.61	0.43	0.64	1.18
	QAMS	1.77	0.43	0.50	2.11	1.58	2.12	0.71	1.66	0.45	1.22	N/A	1.72	1.64	0.62	0.44	0.65	1.19
	RE/%	0.61	0.61	0.71	0.59	0.58	0.59	0.69	0.56	0.62	0.63	N/A	0.59	0.60	0.59	0.68	0.69	0.63
Component 9	ESM	0.28	N/A	N/A	0.79	0.30	0.82	0.25	N/A	N/A	0.77	0.41	0.13	0.33	N/A	N/A	N/A	0.74
	QAMS	0.28	N/A	N/A	0.78	0.30	0.80	0.24	N/A	N/A	0.76	0.40	0.13	0.33	N/A	N/A	N/A	0.73
	RE/%	−1.75	N/A	N/A	−1.92	−1.72	−1.87	−1.89	N/A	N/A	−1.84	−1.91	−1.20	−1.90	N/A	N/A	N/A	−1.86
Component 10	ESM	1.18	0.38	0.46	N/A	1.11	0.15	0.59	0.47	0.51	N/A	N/A	2.87	1.43	0.76	0.46	0.72	0.74
	QAMS	1.18	0.37	0.45	N/A	1.08	0.15	0.57	0.45	0.49	N/A	N/A	2.78	1.38	0.73	0.45	0.70	0.72
	RE/%	−0.20	−0.14	−0.15	N/A	−0.19	0.03	−0.20	−0.22	−0.16	N/A	N/A	−0.19	−0.18	−0.09	−0.07	−0.09	−0.20

[a] N/A: above LOD yet below LOQ, and thus cannot be quantitatively analyzed.

obvious grouping characteristics. S1, S4, S5, S6, S12, S13, and S17 were classified into Group I due to higher contents, while S2, S3, S7, S8, S9, S10, S11, S14, S15, and S16 were classified into Group II as lower contents. This aligns with the HCA results, indicating that the internal quality differences of CA in different batches can be effectively distinguished by the quantitative analysis using such 10 components. It is further evidenced that the overall chemical quality of CA can be efficiently and reliably evaluated by the QAMS method established in this study, with component 5 as the internal reference standard, thereby providing a scientific basis for its quality evaluation. It was worth noting that sample S11, which had shown significant

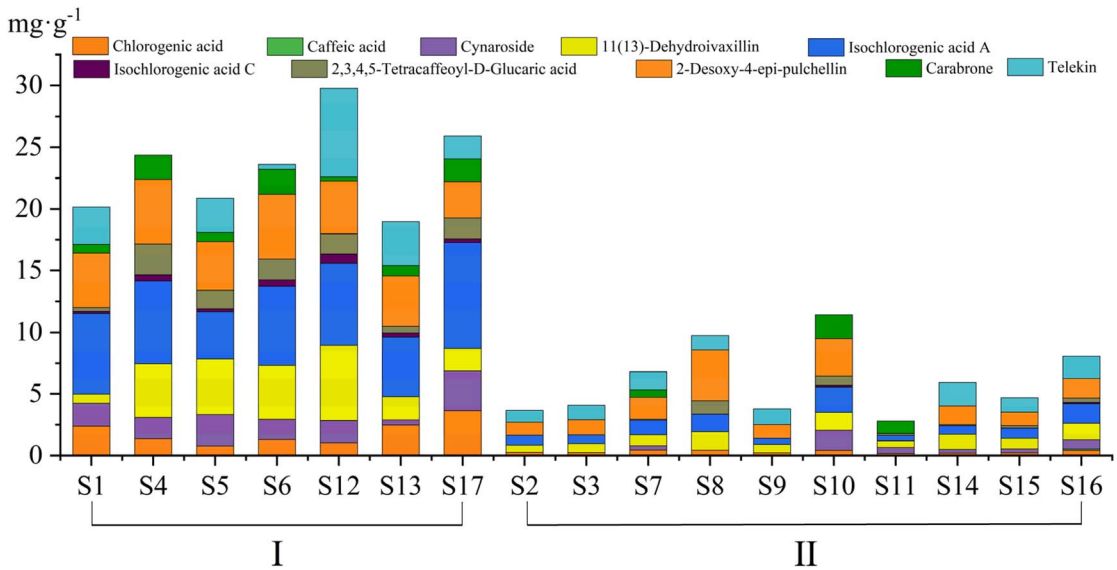

Fig. 5 Stacked chart of the contents of 10 components in 17 batches of CA samples.

© 2026 The Author(s). Published by the Royal Society of Chemistry

Open Access Article. Published on 13 February 2026. Downloaded on 5/20/2026 7:02:52 PM.
This article is licensed under a Creative Commons Attribution-NonCommercial 3.0 Unported Licence.

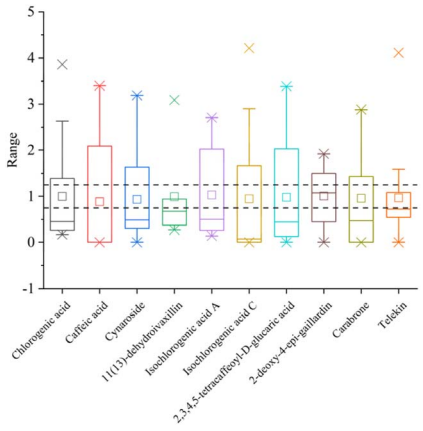

Fig. 6 Box chart of 10 components from 17 samples.

differences in the previous fingerprint similarity analysis (with a similarity of 0.694), also had a relatively low total content of the 10 components. The contents of several key components of sample S11, such as component 5 (0.18 mg g^{-1}), component 7 (0.06 mg g^{-1}), component 1 (0.06 mg g^{-1}), and component 3 (0.2 mg g^{-1}), were far below the average values. Furthermore, the concentrations of some components (such as components 6, 8, and 10) were even below the method's limit of quantification (LOQ) and could not be accurately quantified. This low content of chemical constituents resulted in the deviation of its fingerprint profile from the reference chromatogram, leading to a low similarity coefficient.

3.6.5 Quality fluctuation analysis. *P*-Values quantified batch-to-batch quality fluctuation, with batch consistency characterised by *P*-values of 0.75–1.25.[32,49] The results were illustrated in Fig. 6. The interquartile range (25–75th percentiles) of components 1, 2, 3, 5, 6, 7, 8, and 9 surpassed acceptable thresholds, signifying that these outliers were important components influencing the quality fluctuations of the 17 batches of CA samples. Notably, these components are also the primary bioactive constituents of CA. For instance, the identified phenolic acids are known to regulate ROS and MMP-1 overproduction and exhibit significant antimicrobial effects,[50] while sesquiterpenoids like component 9 and flavonoids like component 3 possess potent anti-inflammatory and antioxidant activities.[51,52] The integration of quality fluctuation and clustering analysis indicates that the first group of samples, characterized by high levels of these 8 components, exhibits better quality, which may be related to the content of the active ingredients.

4 Conclusions

This study established an integrated strategy that combines UPLC fingerprinting, chemometrics, and quantitative analysis of QAMS for a thorough quality evaluation of CA. The UPLC fingerprint revealed 19 common peaks, which were identified by UPLC-Q-TOF-MS, achieving effective separation of multiple components, such as sesquiterpenoids, phenolic acids, and flavonoids. 10 components were selected as quantitative components based on their high abundance and well-documented anti-inflammatory, antioxidant, and antibacterial properties.[6–8,53–58] Chemometric analyses (HCA, PCA, and OPLS-DA) effectively classified the samples and screened out differential components, demonstrating the capability of this method to reveal the chemical characteristics of CA.

Significantly, a QAMS method was developed using low-cost and readily available isochlorogenic acid A as the internal reference. Although the slope-based ratio method is an emerging trend, our validation confirmed that within the linear range, the classic single-point method adopted in this study was mathematically equivalent and equally accurate, while being more concise and aligned with pharmacopoeial standards. The method validation demonstrated excellent repeatability, stability, and precision. The quantitative results obtained by QAMS showed no significant difference from those of the traditional external standard method, proving its reliability without the need for multiple expensive standards.

In conclusion, in this paper, a strategy combining UPLC fingerprint, chemometrics and QAMS was successfully established and applied for the first time to evaluate the quality of CA, filling the gap in the standardized quality research of CA. The established qualitative and quantitative methods were simple, rapid, and cost-effective, which could provide a reference for the quality control and evaluation of this medicinal herb.

Author contributions

Conceptualization, J. Yan and J. Yang; data curation, and writing—original draft preparation, J. Yang, Y. Zhang; software, X. Hu; writing—review and editing, Y. Wang, J. Yu, P. Fu.; funding acquisition, Y. Wang, J. Yan, S. Li. All authors have read and agreed to the published version of the manuscript.

Conflicts of interest

There are no conflicts to declare.

Data availability

The data supporting this article have been included as part of the supplementary information (SI). Supplementary information: Fig. S1, UPLC-Q-TOF-MS chromatogram of CA in positive and negative ion modes. Table S1, system suitability test of RCFs. Table S2, relative retention time of each component. See DOI: https://doi.org/10.1039/d6ra00067c.

Acknowledgements

This research was funded by Xiangxi Prefecture Technical Tackling "Reveal the List and Take Command" Project (2022JBGS0003), Key Discipline Project on Chinese Pharmacology of Hunan University of Chinese Medicine (202302), and Hunan University of Chinese Medicine Graduate Student Innovation Project (2024CX080).

Open Access Article. Published on 13 February 2026. Downloaded on 5/20/2026 7:02:52 PM. This article is licensed under a Creative Commons Attribution-NonCommercial 3.0 Unported Licence.

References

1 L. Wang, W. Qin, L. Tian, X. Zhang, F. Lin, F. Cheng, J. F. Chen, C. X. Liu, Z. Guo, P. Proksch and K. Zou, *Fitoterapia*, 2018, **127**, 349–355.

2 Hunan Provincial Food and Drug Administration, *Hunan Provincial Specification for the Processing of Traditional Chinese Medicine Decoction Pieces*. Hunan Science and Technology Press, Changsha, China, 2021, p. , p. 353.

3 X. Chai, Y. Le, J. Wang, C. Mei, J. Feng, H. Zhao, C. Wang and D. Lu, *J. Food Sci.*, 2019, **84**(12), 3825–3832.

4 S. R. M. Ibrahim, S. A. Fadil, H. A. Fadil, R. H. Hareeri, H. M. Abdallah and G. A. Mohamed, *Plants*, 2022, **11**(12), 1598.

5 Y. F. Wang, Y. Fu, Y. N. Ji, N. N. Shi, F. Sauriol, X. H. Lu, Y. C. Gu, Q. W. Shi and C. H. Huo, *Phytochemistry*, 2022, **203**, 113389.

6 L. Fu, C. C. Wang, W. Tian, Z. Liu, M. Y. Bao, J. Liu, W. Zhang, L. P. Bai, Z. H. Jiang and G. Y. Zhu, *J. Nat. Prod.*, 2024, **87**(7), 1786–1797.

7 X. F. Zhang, H. F. Li, H. Liu, F. L. Wei, J. X. Du, J. K. Liu, J. He and T. Feng, *Bioorg. Chem.*, 2024, **151**, 107684.

8 L. Li, S. Yang, D. Chen, Z. Wu, M. Zhang, F. Yang, L. Qin and X. Zhou, *Molecules*, 2022, **27**(23), 8313.

9 J. Wu, C. Tang, L. Chen, Y. Qiao, M. Geng and Y. Ye, *Org. Lett.*, 2015, **17**(7), 1656–1659.

10 S. B. Lee, K. Kang, H. J. Lee, J. H. Yun, E. H. Jho, C. Y. Kim and C. W. Nho, *J. Med. Food*, 2010, **13**(1), 39–46.

11 L. Tian, F. Cheng, L. Wang, W. Qin, K. Zou and J. Chen, *Molecules*, 2019, **24**(6), 1091.

12 X. Zhang, M.-J. Han, X. Y. Han, J. H. Jia, R. Y. Lu, G. D. Yao, Y. Y. Liu, M. Bai and S. J. Song, *Fitoterapia*, 2024, **175**, 105947.

13 S. J. Woo, M. G. Jeong, E. J. Jeon, M. Y. Do and N. Y. Kim, *Comp. Biochem. Physiol., Part C:Toxicol. Pharmacol.*, 2022, **251**, 109214.

14 Q. Liang, X. Yang, D. Liao, C. Yi, R. Dang, J. Wu and L. Huang, *J. Visualized Exp.*, 2022, **186**, e63976.

15 J. T. Feng, H. Wang, S. X. Ren, J. He, Y. Liu and X. Zhang, *J. Agric. Food Chem.*, 2012, **60**(15), 3817–3823.

16 A. Haris, M. Azeem and M. Binyameen, *J. Med. Entomol.*, 2022, **59**(3), 801–809.

17 Y. W. Fan, Z. Y. Ao, W. J. Zhang, J. Y. Chen, X. Lian, P. Y. Chen, L. P. Chen, J. W. Wu and J. Yuan, *Nat. Prod. Res.*, 2024, **38**(11), 1909–1917.

18 Y. W. Fan, W. J. Zhang, Z. Y. Ao, J. Y. Chen, X. Lian, Y. C. Pan, L. P. Chen, D. X. Jiang and J. W. Wu, *Fitoterapia*, 2023, **169**, 105548.

19 J. W. Wu, C. P. Tang, S. Yao, C. Q. Ke and Y. Ye, *Chin. J. Nat. Med.*, 2021, **19**(11), 868–873.

20 B. J. Yang, J. Wang, Z. Q. Zeng, X. Yang, A. Y. Huang, X. J. Hao, X. Ding and S. L. Li, *Nat. Prod. Res.*, 2022, **36**(12), 3207–3210.

21 Q. Wang, L. H. Pan, L. Lin, R. Zhang, Y. C. Du, H. Chen, M. Huang, K. W. Guo and X. Z. Yang, *Curr. Med. Sci.*, 2018, **38**(6), 1045–1053.

22 M. Liu and X.-J. Zhou, *Zhongguo Zhongyao Zazhi*, 2015, **40**(09), 1783–1786.

23 C. Su, Y. Xie, B. Wang, L. Cui, B. Liu, Y. Zhou, S. Yang, L. Zhang and Y. Xu, *Sci. Rep.*, 2025, **15**(1), 5810.

24 Y. Li, X. Wu, Y. Ma, L. Xu, C. Yang, D. Peng, X. Guo and J. Wei, *Front. Chem.*, 2024, **11**, 1309965.

25 J. Wu, L. Wang, Y. Cui, C. Liu, W. Ding, S. Ren, R. Dong and J. Zhang, *Molecules*, 2024, **29**(19), 4600.

26 X. Cao, M. Li, L. Ma, M. Wang, X. Hou and M. Maiwulanjiang, *Molecules*, 2022, **27**(9), 2634.

27 Z. Guo, Y. Duan, Z. Zhao, D. Yang and X. Xu, *Pharmaceuticals*, 2024, **17**(3), 313.

28 R. Xu, F. Mao, Y. Zhao, W. Wang, L. Fan, X. Gao, J. Zhao and H. Tian, *Molecules*, 2017, **22**(12), 2276.

29 FDA, *Botanical Drug Development Guidance for Industry*, U.S. Food and Drug Administration, Silver Spring, MD, USA, 2016.

30 EMA, *Guideline on Quality of Herbal Medicinal Products/ Traditional Herbal Medicinal Products*. European Medicines Agency, Amsterdam, The Netherlands, 2022.

31 D. W. Li, M. Zhu, Y. D. Shao, Z. Shen, C. C. Weng and W. D. Yan, *Food Chem.*, 2016, **197**, 1112–1120.

32 Y. Lei, Y. Wang, Z. Sun, M. Lin, X. Cai, D. Huang, K. Luo, S. Tan, Y. Zhang, J. Yan and X. Xia, *J. Sep. Sci.*, 2020, **43**(7), 1382–1392.

33 X. Wang, Q. Jia, X. Yao, L. Yang, K. Pei, L. Guo, Y. Guo, Y. Yang and N. Qin, *Food Chem.*, 2025, **462**, 141002.

34 Y. Tian, Q. Li, X. Zhou, Q. Pang and Y. Xu, *J. Chromatogr. B: Anal. Technol. Biomed. Life Sci.*, 2017, **1046**, 1–12.

35 M. J. Rao, B. Feng, M. H. Ahmad, M. Tahir Ul Qamar, M. Z. Aslam, M. F. Khalid, S. Hussain, R. Zhong, Q. Ali, Q. Xu, C. Ma and L. Wang, *Front. Plant Sci.*, 2023, **14**, 1150854.

36 Q. Mu, Y. Bai, J. Qi and C. Sa, *RSC Adv.*, 2025, **15**(33), 27096–27112.

37 K. Gong, Y. Yang, K. Li, L. Zhu, X. Zhi and W. Cai, *Pharm. Biol.*, 2020, **58**(1), 992–998.

38 S. Schwaiger, C. Seger, B. Wiesbauer, *et al.*, *Phytochem. Anal.*, 2006, **17**(5), 291–298.

39 F. Wang, K. Yang, F. Ren and J. Liu, *Fitoterapia*, 2009, **80**, 21–24.

40 Q. Hu, P. Wu, Y. Liu, F. Qi, C. Yu, Y. Zhao, Y. Yu, D. Fei and Z. Zhang, *Phytochem. Lett.*, 2018, **27**, 154–159.

41 L. Wang, W. Qin, L. Tian, X. Zhang, F. Lin, F. Cheng, J. Chen, C. Liu, Z. Guo and P. Proksch, *Fitoterapia*, 2018, **127**, 349–355.

42 B. Yang, J. Wang, Z. Zeng, X. Yang, A. Huang, X. Hao, X. Ding and S. Li, *Nat. Prod. Res.*, 2022, **36**(12), 3207–3210.

43 M. Zhu, Z. F. Zhou, X. P. Wu, R. P. Liu, J. J. Zheng, J. L. Wang and J. X. Wan, *Ecol. Indic.*, 2024, **158**, 111495.

44 Y. J. Yan, Q. H. Dai, L. Jin and X. D. Wang, *Catena*, 2019, **174**, 48–58.

45 T. Luo, Z. T. He, D. Xia, Y. K. Xu, L. Xia, T. Guo, W. N. Xu and J. Fang, *Environ. Technol. Innovation*, 2025, **38**, 104074.

46 M. Karim, O. Beyan, A. Zappa, I. Costa, D. Rebholz-Schuhmann, M. Cochez and S. Decker, *Briefings Bioinf.*, 2021, **22**, 393–415.

© 2026 The Author(s). Published by the Royal Society of Chemistry

Open Access Article. Published on 13 February 2026. Downloaded on 5/20/2026 7:02:52 PM.
This article is licensed under a Creative Commons Attribution-NonCommercial 3.0 Unported Licence.

47 X. Long, R. Li, H. Liu, Z. Xia, S. Guo, J. Gu, L. Zhang, Y. Fan and Z. Chen, *Phytochem. Anal.*, 2023, **34**(4), 476–486.
48 P. Wang, J. Zhang, Y. Zhang, H. Su, X. Qiu, L. Gong, J. Huang, J. Bai, Z. Huang and W. Xu, *RSC Adv.*, 2019, **9**(40), 23373–23381.
49 F. Gao, Z. Xu, W. Wang, G. Lu, H. Y. Vander, T. Zhou and G. Fan, *J. Chromatogr. A*, 2016, **1466**, 67–75.
50 S. R. Son, K. S. Kim, D. S. Jang and S. Lee, *J. Agric. Food Chem.*, 2025, **73**(22), 13471–13487.
51 L. Han, S. Sun, Y. Yang, Y. Chen, G. Dong, T. Li, Y. Li and L. Zhang, *Curr. Res. Food Sci.*, 2025, **11**, 101256.
52 A. De Stefano, S. Caporali, N. Di Daniele, V. Rovella, C. Cardillo, F. Schinzari, M. Minieri, M. Pieri, E. Candi, S. Bernardini, M. Tesauro and A. Terrinoni, *Int. J. Mol. Sci.*, 2021, **22**(3), 1321.
53 A. Pan, J. Jin, Y. Wu, Q. Zhang, H. Chen, Y. Hu, W. Xiao, A. Shi, Y. Yang, L. Jiang, M. Tan, J. Wang and L. Hu, *MedComm*, 2025, **6**(3), e701.
54 X. Xiao, H. Li, H. Jin, J. Jin, M. Yu, C. Ma, Y. Tong, L. Zhou, H. Lei, H. Xu, W. Zhang, W. Liu and Y. Wu, *Cell Death Dis.*, 2017, **8**(9), e3050.
55 N. Sławińska, M. Kluska, B. Moniuszko-Szajwaj, A. Stochmal, K. Woźniak and B. Olas, *Nutrients*, 2023, **15**(7), 1671.
56 M. Naveed, V. Hejazi, M. Abbas, A. A. Kamboh, G. J. Khan, M. Shumzaid, F. Ahmad, D. Babazadeh, X. Fangfang, F. Modarresi-Ghazani, L. Wenhua and Z. Xiaohui, *Biomed. Pharmacother.*, 2018, **97**, 67–74.
57 M. D. S. S. Chagas, M. D. Behrens, C. J. Moragas-Tellis, G. X. M. Penedo, A. R. Silva and C. F. Gonçalves-de-Albuquerque, *Oxid. Med. Cell. Longevity*, 2022, **2022**, 9966750.
58 D. Stefano, S. Caporali, N. Di Daniele, V. Rovella, C. Cardillo, F. Schinzari, M. Minieri, M. Pieri, E. Candi, S. Bernardini, M. Tesauro and A. Terrinoni, *Int. J. Mol. Sci.*, 2021, **22**(3), 1321.

© 2026 The Author(s). Published by the Royal Society of Chemistry